Hindawi
Molecular Imaging
Volume 2023, Article ID 7855924, 11 pages
https://doi.org/10.1155/2023/7855924

Research Article

13-*cis*-Retinoic Acid Affects Brain Perfusion and Function: In Vivo Study

Fatma Al-Saeedi[1] **and Peramaiyan Rajendran**[2,3]

[1]*Nuclear Medicine, Faculty of Medicine, Kuwait University, Kuwait City, Kuwait*
[2]*Department of Biological Sciences, College of Science, King Faisal University, Al-Ahsa 31982, Saudi Arabia*
[3]*Centre of Molecular Medicine and Diagnostics (COMManD), Department of Biochemistry, Saveetha Dental College & Hospitals, Saveetha Institute of Medical and Technical Sciences, Saveetha University, Chennai, 600 077 Tamil Nadu, India*

Correspondence should be addressed to Fatma Al-Saeedi; fatma.alsaeedi@ku.edu.kw

Received 23 August 2022; Revised 3 January 2023; Accepted 12 January 2023; Published 13 February 2023

Academic Editor: Ali Azhdarinia

Purpose. Study the effects of 13-cis-retinoic acid (13-RA), a synthetic analogue of a vitamin A used for the treatment of severe acne, on the blood flow in the rat brain using technetium-99m hexamethyl propylene amine oxime (^{99m}Tc-HMPAO) imaging. *Methods*. A total of 30 adult male Wistar rats were divided into the control (C), low-dose (L), and high-dose (H) groups. The L and H rats were exposed subcutaneously to 0.3 and 0.5 mg, respectively, of 13-RA per kg of body weight for seven days. Brain blood flow imaging was performed using a gamma camera. Then, a region of interest (ROI) around the brain (target, T), a whole-body region (WB), and a background region (BG) was selected and delimited. The net ^{99m}Tc-HMPAO brain counts were calculated as the net target counts, NTC = (T − BG)/(WB − BG) in all groups. At the end of the ^{99m}Tc-HMPAO brain blood flow imaging, the brain, heart, kidney, lung, and liver were rapidly removed, and their uptake was determined. Brain histopathological analysis was performed using hematoxylin and eosin stains. In addition, the plasma fatty acids were studied using gas chromatography/mass spectrometry. *Results*. There were highly significant differences between L and H in comparison to C and across the groups. The ^{99m}Tc-HMPAO radioactivity in the brain showed increased uptake in a dose-dependent manner. There were also significant changes in the brain tissues and decreased free fatty acids among the groups compared to C. *Conclusion*. 13-RA increases ^{99m}TcHMPAO brain perfusion, uptake, and function and reduces fatty acids.

1. Introduction

Isotretinoin (13-cis-retinoic acid, 13-RA), a vitamin A derivative (retinoid), is commonly prescribed for severe acne that is resistant to other treatments [1]. It has been effective in the clinical control of acne. However, it has a wide range of side effects, such as teratogenesis in gestation [2, 3], arthritis [4], sacroiliitis with severe disability [5], liver damage [6], and psychosocial symptoms such as anxiety, depression, disturbance in satisfaction, and quality of life [7, 8]. Some studies reported that the administration of 13-RA can cause physiological changes that are pathways for the pathology of different psychiatric conditions such as increased oxidative stress [6, 9, 10], headache, seizures, confusion, and cerebral ischemia [11]. Consequently, stress is believed to be the root cause of any central nervous system disorder such as depression. Some experimental approaches have shown hypothalamo-pituitary-adrenal (HPA) axis stimulation in stress-induced disruption of the BBB. The BBB is the neurovascular unit that controls the transition of matter and blood-borne immune cells into the brain parenchyma. Plus, the BBB prevents any peripheral injury to the brain tissue or its material.

Persons who use 13-RA to treat acne can develop mood swings such as cognitive neuropsychological disturbances, stress-induced mood swings, anxiety, amnesia, insomnia, and depression as well as suicide ideation or even suicide itself [12–15]. The pathogenic mechanism is unknown. It is

known, however, that 13-RA affects steroid production in rats [16] and that many steroids can cause mood swings in humans [17, 18] and vasodilation [19, 20]. The mechanism behind these changes lies in the ability of isotretinoin to regulate gene expression in the brain [13, 21].

Few studies have also shown a relationship between 13-RA treatment and stress in general and between 13-RA treatment and the brain as a specific organ. This study investigated if 13-RA treatment in rats would affect their brain blood flow. Therefore, a rat model was used to determine if 13-RA administration induces stress. Many studies have used rat models for stress [22, 23] because they have similar characteristics to humans in their expression of emotions [24, 25]. In an experiment on rats, chronic unpredictable mild stress (CUMS) induced depressive-like behaviors [25, 26].

In nuclear medicine, technetium-99m hexamethyl propylene amine (^{99m}Tc-HMPAO) is used as a radiotracer for investigating regional cerebral blood flow in humans. It is potentially useful for assessing cerebral blood flow in small animals [27, 28] and in several disease models [29, 30]. It has also been used to label leukocytes for the detection of inflammation [31, 32]. Scientists believe that ^{99m}Tc-HMPAO accumulates in the brain through its intracellular conversion from a lipophilic form to a hydrophilic form in the brain parenchyma [33].

2. Materials and Methods

2.1. Materials. The HMPAO pharmaceutical kit (exametazime) was purchased from GE Healthcare (Chalfont St. Giles, UK). The 99m-technetium pertechnetate (99m Tc-pertechnetate, $^{99m}TcO^{-4}$) radionuclide was obtained from a molybdenum99-technetium-99 m ($^{99}Mo^{99m}Tc$) generator purchased from Amersham International PLC (Amersham, UK). The following authentic lipids were purchased from Sigma (St. Louis, Mo, USA): fatty acids (palmitic acid (C16:0), pentadecanoic acid (C15:0), adrenic acid (C22:4), docosapentaenoic acid (C22:5), and cervonic acid (docosahexaenoic acid; C22:6)); cholesterol heptadecanoate; heptadecanoyl CoA; tripalmitin; and D-α-Phosphatidylcholine, dipalmitoyl. Intraval sodium (thiopental sodium) was purchased from Panpharma UK Ltd (Southport, UK). The BF-3 methanol derivatization kit was purchased from Supelco (Bellefonte, USA).

2.2. Experimental Animals and Ethics Statement. Adult male Wistar rats ($n = 30$), each of which weighed 200 g, were handled in accordance with ethical standards. All experiments were performed according to the ethical guidelines set out in the Guide for the Care and Use of Laboratory Animals and with the approval of the Ethics Committee of the Animal Resources Centre of Kuwait University's Faculty of Medicine. All the animals had free access to water and food. The environment of the animal room was carefully controlled, with a 12 h dark/light cycle, a temperature of 20°C, and a humidity of 45%.

2.3. ^{99m}Tc-HMPAO Labeling. The labeling procedure was performed following the manufacturer's instructions. 2,960 MBq of 99m Tc-pertechnetate in 3 ml saline was added to a freeze-dried exametazime kit to prepare ^{99m}Tc-HMPAO. In all cases, the labeled ^{99m}Tc-HMPAO was fresh and used within 30 min from the time of its preparation. Its radiochemical purity was verified through thin-layer chromatography according to the manufacturer's recommendations and ranged from 95% to 99%.

2.4. Experiment Protocol. The rats were randomly divided into three groups: the control group (C), which was given 0 mg of 13-RA per kg of body weight; the low-dose group (L), which was given 0.3 mg/kg of 13-RA; and the high-dose group (H), which was given 0.5 mg/kg of 13-RA. The dose of 13-RA was dissolved in 2 ml DMSO and suspended in 2 ml propylene glycol. Each rat received the dose subcutaneously for seven consecutive days, after which their brain blood flow was immediately and dynamically studied using ^{99m}Tc-HMPAO imaging. Control animals received subcutaneous injections of 0.5 ml saline solution (pH 8.6). Ten minutes prior to imaging, each rat was anesthetized through intraperitoneal injection of 25 mg/kg intraval sodium. Then, an intravenous line was inserted into the tail vein of each rat, after which each rat was transferred to and fixed on a fixed board against the table of the gamma camera. The rat was positioned so that its head was localized at the center of the field of view. Then, it was injected with 125 MBq of ^{99m}Tc-HMPAO intravenously, followed by a saline push during the brain image acquisition. The acquisition lasted 60 min and was captured in images with the gamma camera for the entire experiment.

2.5. ^{99m}Tc-HMPAO Brain Flow Gamma Camera Imaging. To study the brain blood flow, the injected rats were imaged. Each scan was performed using a single-head gamma (γ) camera (Philips camera; Odyssey LX) equipped with a high-resolution parallel hole collimator connected to a Dell computer. The matrix was 64×64 pixels, and the photopeak was focused at 140 keV with a symmetric 10% window. A zoom factor of 4 was applied during each acquisition time. Dynamic whole-body imaging was performed in two phases: (1) the vascular phase at 1 sec/frame for 3 min, followed by (2) the parenchymal phase at 1 min/frame for 60 min after the ^{99m}Tc-HMPAO injection.

2.6. Image Processing. The brain scans and frame data were collected and combined in one frame. Then, the region of interest (ROI) around the brain (target, T), the whole-body region (WB), and the background soft tissues of the rat (BG) was delimited. The net ^{99m}Tc-HMPAO uptake of the brain was calculated as the net target count, $NTC = (T - BG)/(WB - BG)$, in each of the groups and was expressed as the mean ± standard deviation (mean ± SD). The ROIs were drawn with equal pixel sizes to avoid discrepancies among the groups.

2.7. ^{99m}Tc-HMPAO Uptake. After imaging, the rats were euthanized by cervical dislocation to collect their blood, heart, lung, brain, kidneys, liver, gut, bone, adrenals, and testes for further study. The rats from each group were resected, and the respective organs were counted in

kilobecquerels (kBq) using a dose calibrator. The counts were recorded and expressed as the mean ± SD and compared with the control. The measured radioactivity from each organ was normalized to the whole body, corrected by the background counts, and expressed as a percentage of the total radioactivity.

2.8. Brain Blood Flow Quantification. In three experiments, for each group (C, L, and H), the cerebral blood flow was quantified using the method done by Hale et al. [34] with minor modifications using colored microspheres. In brief, the 12 μm microspheres (1×10^6) were intravenously injected, collected (0.4 ml/min), isolated by centrifugation, and then counted using an inverted microscope and a hemocytometer (Leica Microsystems, Germany). This is to prove that the brain scan images reflect the cerebral blood flow. Brain blood flow was calculated using the following equation: blood flow (ml/100 g tissue/min) = [(fluorescent intensity in tissue/fluorescent intensity in reference blood) × blood sampling rate (ml/min)] × 100/tissue weight (g).

2.9. Histological Studies and Brain Damage Scoring. Brain light microscopy and histology were performed on a total of three rats from each group. After each animal was sacrificed, 4 ml of blood was collected. The animal's body was perfused with normal saline accompanied by a cold fixative (4% paraformaldehyde and 0.1% glutaraldehyde in 0.1-M PO4 buffer, pH 7.3). After perfusion, 5 mm tissue samples of the brain were collected, placed in the fixative for 24 h, and washed in 0.1 M PO4 buffer for 72 h. Then, the samples were dried in graded ethanol and cleared in xylene using an automatic processor, after which they were embedded in paraffin wax. Thin, 5 μm long sections were cut and stained using hematoxylin and eosin (HE) and cresyl violet stain. The slides were examined under an Olympus microscope BX 41 (USA) with ×40 histopathology magnification. Brain damage was scored following Eşrefoğlu et al. [35] by grading vacuolization; neuronal necrosis; neuronophagia; neuronal perinuclear, interstitial, and perivascular edema; intracerebral and subarachnoid hemorrhage; congestion; and cell infiltration with a maximum score of 20. The scores were 0 for no brain damage, 1 for mild brain damage, 2 for moderate brain damage, and 3 for severe brain damage.

2.10. Modified Unpredictable Mild Stress Model. The unpredictable mild stress model was followed, as described by [36–38], with timing modifications. The remaining animals assigned to the stress group were exposed to one dose of 0.4 mg/kg of 13-RA subcutaneously for seven consecutive days compared to C group, which was given 0 mg of 13-RA per kg of body weight. The control animals were manipulated in a separate room at the same start and end times of the restraint session. All animal groups were regularly provided food and water. After seven days, the animals were not given water a day before the conduct of the sucrose preference test (SPT), as described in [39, 40]. The rats were kept in their assigned cages with free access to two bottles, one of which contained 300 ml of sucrose solution (1%, *w*/*v*) and the other 300 ml of pure water. The weight of each bottle was measured before and after the test. After the test, the SPT was computed as follows: sucrose preference (%) = sucrose consumption/(total consumption [sucrose + water]) × 100%.

2.11. Adrenocorticotropic Hormone (ACTH) and Lipid Adrenal Measurement for Stress. In this study, we used two groups: the control group, which, as mentioned, received 0 mg/kg 13-RA, and the ACTH group, which was given 0.4 mg/kg 13-RA subcutaneously for seven consecutive days. Three milliliters of adrenal homogenates was mixed with a solution that contained 850 mM sucrose (5 mg wet weight/ml), centrifuged at 3,600 rpm (1,452 g), then assayed and analyzed for fatty acids according to the validation protocol of fatty acid quantification, the extraction ratio, hydrolysis, and the methylation efficacy, which was originally established by Ingalls et al. [41], and used in this study with the volume modifications [42, 43].

2.12. Study of Plasma Free Fatty Acids via Gas Chromatography/Mass Spectrometry (GC/MS). Rat lipid samples at a volume of 0.25 ml were used to measure the number of unesterified (free) fatty acids. Each sample was vortexed vigorously for 1 min and then centrifuged at 3,000 rpm (1,615 g) for 10 min at room temperature using an MSE Mistral 2000 centrifuge (with a 4 × 200 swing rotor). The supernatant was collected and transferred to a test tube and dried under a stream of nitrogen gas [44]. The dried lipid extract was resuspended in 200 μl ethanol and subjected to hydrolysis in 200 μl ethanol that contained 1 M KOH at 75°C for 30 min. The hydrolytic reaction was stopped by adding eight drops of 5% HCl (*v*/*v*), and the hydrolyzate was diluted with 200 μl of distilled water. The mixture was reextracted with 1.6 ml of the organic solvent mixture. The pellet was collected and transferred to a test tube and dried under a stream of nitrogen gas. To prepare the fatty acid methyl esters, the dried lipid extract was resuspended in 500 μl of hexane, which was added 500 μl BF3-methanol reagent. After the mixture was heated at 60°C for 3 min precisely, the derivatization was terminated by chilling the test tube in ice and adding 1 ml of ice-chilled (HPLC-grade) water to the mixture. The newly formed fatty acid methyl esters were extracted with 1 ml of hexane, and the hexane layer was dried under a stream of nitrogen gas. The fatty methyl ester mixture was resuspended with 50 μl of isooctane and analyzed using a GC/MS instrument (Shimadzu GC/MS-QP5050A) with a SUPELCO-fused silica capillary column with a 30 m × 0.25 mm × 0.25 μm film thickness (Col. 21205-01A). This time-controlled derivatization technique permitted the determination of methyl esters derived from unesterified fatty acids.

2.13. Data Presentation and Statistical Analysis. All data, unless otherwise stated, were expressed as the mean ± SD. The bar chart data presented are means ± SD. The significance (*p* values) between two groups, such as the experimental and control groups, was determined via Student's *t*-test (unpaired multiple comparison). One-way analysis of variance (ANOVA) was used to evaluate statistical differences

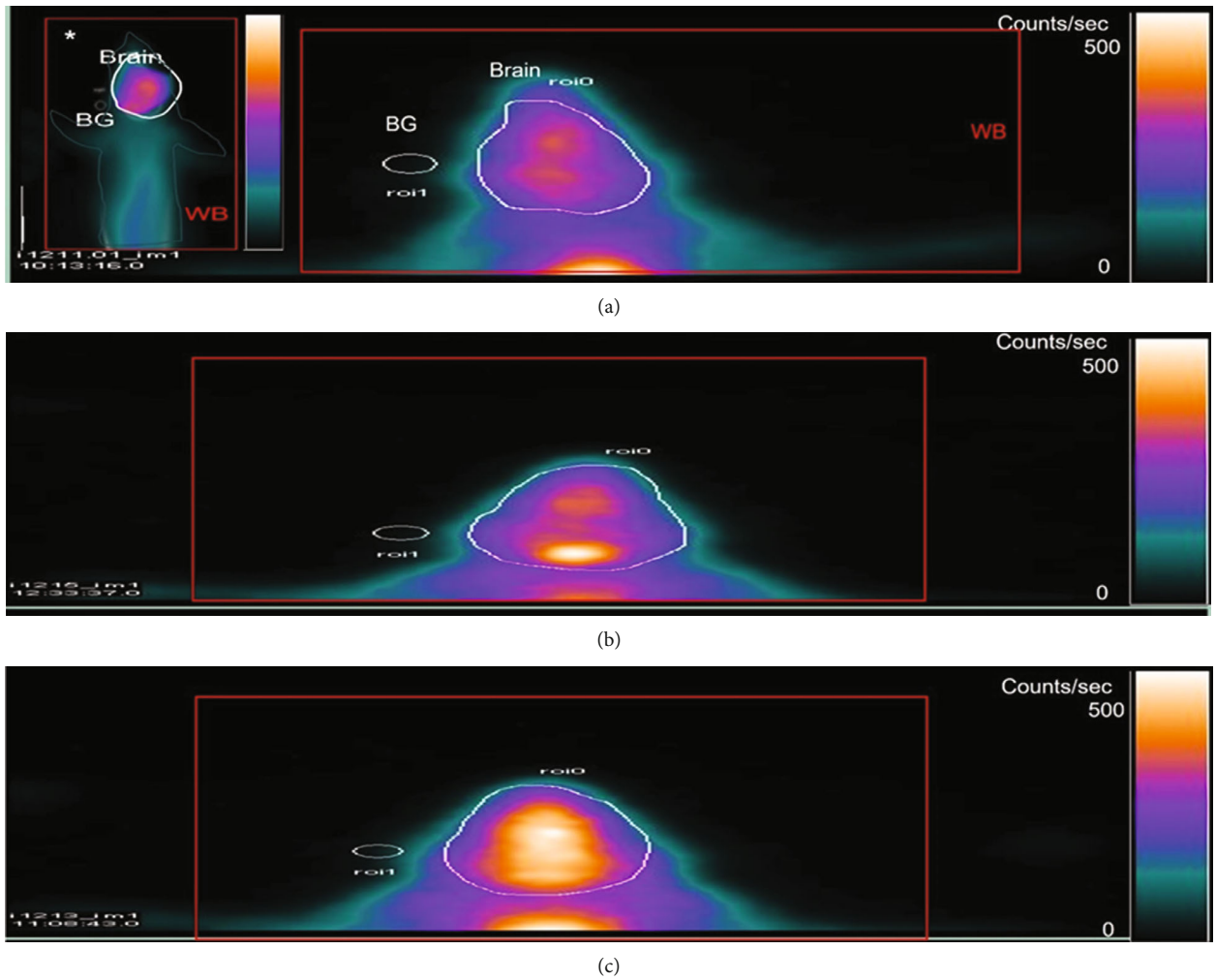

Figure 1: ^{99m}Tc-HMPAO (brain) male rat imaging. Composite 0–60 min images and regions of interest (ROIs) used as (a) receiving 0 mg/kg 13-RA as the control (C), (b) receiving 0.3 mg/kg 13-RA as the low-dose group (L), and (c) receiving 0.5 mg/kg 13-RA as the high-dose group (H). Brain ROI: BG: background and WB: whole body (* whole body of rat image).

between different study groups, such as between three or more experimental groups. A p value < .05 was considered statistically significant. Statistical analysis was performed using SPSS version 13.0 software (IBM SPSS Statistics, 2021).

3. Results

3.1. Analysis of the Brain Radioactivity Concentration. The results showed that the brain radioactivity concentration after the intravenous administration of ^{99m}Tc-HMPAO was steady 30–60 min postinjection. The uptake was determined using the ROI around the T to WB ratio. The next T count, NTC, showed increased uptake (to double) in a dose-dependent manner. Figure 1 shows the images of the ^{99m}Tc-HMPAO (brain) male rats. The composite 0–60 min image and the ROIs were used as C, L, and H groups. The unpaired multiple comparison tests showed highly significant differences between C and L and H ($p < .0001$). The net ^{99m}Tc-HMPAO brain NTCs in C, L, and H (mean ± SD) were 231.8 ± 9.5, 363.6 ± 9.0, and 462 ± 10.3, respectively. The ANOVA showed highly significant statistical differences between the means of the three independent groups. The f-ratio value was 1,407.34849, and the p value was <.00001.

3.2. ^{99m}Tc-HMPAO Uptake. Table 1 shows the resected organs. The uptakes were arranged in descending order from the highest to the lowest uptakes, which were in the brain, kidney, heart, liver, gut, adrenal, lung, testes, blood, and bone. The ANOVA showed p value < .00001, a highly significant ^{99m}Tc-HMPAO brain uptake difference. The ^{99m}Tc-HMPAO brain uptake increased with the 13-RA dose. The brain uptake in L was doubled than that in C, and the brain uptake in H was four times than that in C.

3.3. Brain Blood Flow Quantification. The results of the microsphere method showed the evidence that the composite images at 0-60 min postinjection of ^{99m}Tc-HMPAO reflected cerebral blood flow (CBF). There was a strong correlation ($r = 0.97$) between absolutely quantified CBF (ml/min/g tissue) and the ^{99m}Tc-HMPAO images. In general,

Table 1: ^{99m}Tc-HMPAO uptake for control (C), low-dose 13-RA-injected rats (L), and high-dose 13-RA-injected rats (H).

^{99m}Tc-HMPAO uptake ratio as percentages	C	L	H
Brain	48.27 ± 1.20	67.30 ± 1.23	79.47 ± 1.80
Kidney	22.82 ± 1.05	15.41 ± 1.03	10.27 ± 0.98
Heart	10.94 ± 0.74	6.44 ± 0.65	3.79 ± 0.54
Liver	6.97 ± 0.56	2.61 ± 0.51	0.98 ± 0.45
Gut	3.16 ± 0.53	2.10 ± 0.43	1.40 ± 0.41
Adrenal	2.67 ± 0.40	2.02 ± 0.38	1.33 ± 0.30
Lung	2.10 ± 0.54	2.06 ± 0.32	1.50 ± 0.02
Testes	1.53 ± 0.05	1.17 ± 0.04	0.74 ± 0.03
Blood	1.10 ± 0.05	0.65 ± 0.04	0.38 ± 0.06
Bone	0.44 ± 0.03	0.24 ± 0.02	0.14 ± 0.01

Activity in resected organs, normalized and corrected by background counts and whole-body radioactivity. The values are expressed as percentages. $^{*}p$ value is 0.69 by ANOVA (the f-ratio value is 0.38).

^{99m}Tc-HMPAO brain uptake indicates the semiquantified CBF related to the whole brain or cerebellum CBF (Figure 2). The differences between the three treatment groups were statistically relevant considering that there was a p value of less than 0.05 (3.74008E-06). There was a strong correlation of $r^2 = 0.99$ between C and L, $r^2 = 0.99$ between C and H, and $r^2 = 0.99$ between H and L.

3.4. Histological Changes in the Brain. Figure 3 shows the histological changes of the brain light microscopy of each of the C, L, and H groups using the HE and cresyl violet stain. Figure 3(a) shows a normal rat brain with a uniform and normal arrangement and structure of cerebral capillaries (capillary structure, Cap) and blood vessels with a normal configuration. However, with the use of the 13-RA dose, the L group rats showed increased glycolipids, which signified congestion of the cerebral blood vessels (small arrow) and focal hemorrhage (long arrows). The hippocampal neurons were reduced to ghost cells, with no nuclear staining, a barely visible cell outline, and softening and hemorrhage (chevron arrows). The H group showed necrosis of neurons (small stars), neuronophagia (small circles), and neuronal edema (small crescent shape). In addition, subarachnoid hemorrhage was seen.

3.5. Modified Unpredictable Mild Stress Model. According to the results of the stress model, the stress group showed a highly significant unpaired multiple comparison test result with a $p < .001$ decrease (60% ± 0.60) in the SPT in comparison to C (80% ± 0.52).

3.6. GC/MS. Figure 4 shows the GC/MS results for the free fatty acids in both C and the stress group, indicated by the ACTH adrenal homogenates. There were highly significant differences among the experiment groups in both the unpaired t-test and the ANOVA ($p < .0001$) analysis. There was a highly significant downregulation of the 16:0-palmitate, 18:2-linoleate, 18:1-oleate, 18:0-stearate, 20:4-arachidonate, 22:6-docosahexaenate, and 22.04-docosatetraenoate fatty acids in comparison to C.

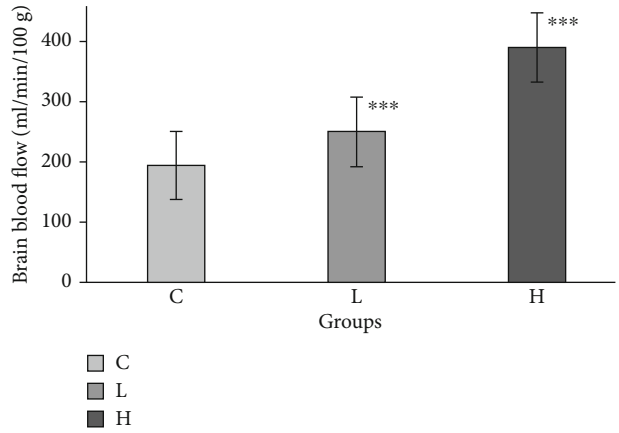

Figure 2: Quantification of cerebral blood flow using the microsphere method. C: control group receiving 0 mg/kg 13-RA; L: low-dose group receiving 0.3 mg/kg 13-RA; H: high-dose group receiving 0.5 mg/kg 13-RA.

4. Discussion

The main objective of this study was to investigate the relationship between stress and 13-RA treatment. It was hypothesized that 13-RA treatment affects brain blood flow, thus playing a role in the development of depression. The study was conducted by imaging brain perfusion in rat models treated with 13-RA.

Our results showed that 13-RA increases blood flow, perfusion, and uptake in rat brain in a dose-dependent manner. Our study presents evidence for the experimental design that composite images at 0–60 min reflected the brain or cerebral blood flow (CBF). The well-known microsphere method absolutely quantified CBF (ml/min/g tissue) [45–47] and correlated strongly with the ^{99m}Tc-HMPAO radioactivity images and results. Even, the results of the ^{99m}Tc-HMPAO brain uptake in the L group increased to twice that in the control, and the brain uptake in the H group was fourfold that in the control.

These results posit that ^{99m}Tc-HMPAO uptake reflects the CBF, which is related to the whole brain or cerebellum CBF. This agrees with many studies that illustrate changes in regional CBF are reflected in parallel to the changes in the ^{99m}Tc-HMPAO retention and uptake [48–53], as well as cerebral metabolism.

There were also observations relative to brain histology in the C, L, and H groups. The histological changes of the brain light microscopy of each of the C, L, and H groups with the use of the 13-RA dose showed increased glycolipids, signifying the congestion of the cerebral blood vessels, focal hemorrhage, and soft neurons in the L group. Similar changes were observed in the H group such as neuronal edema and necrosis, neuronophagia, and subarachnoid hemorrhage.

These results therefore proved that 13-RA caused the inhibition of neurogenesis. This has been hypothesized to

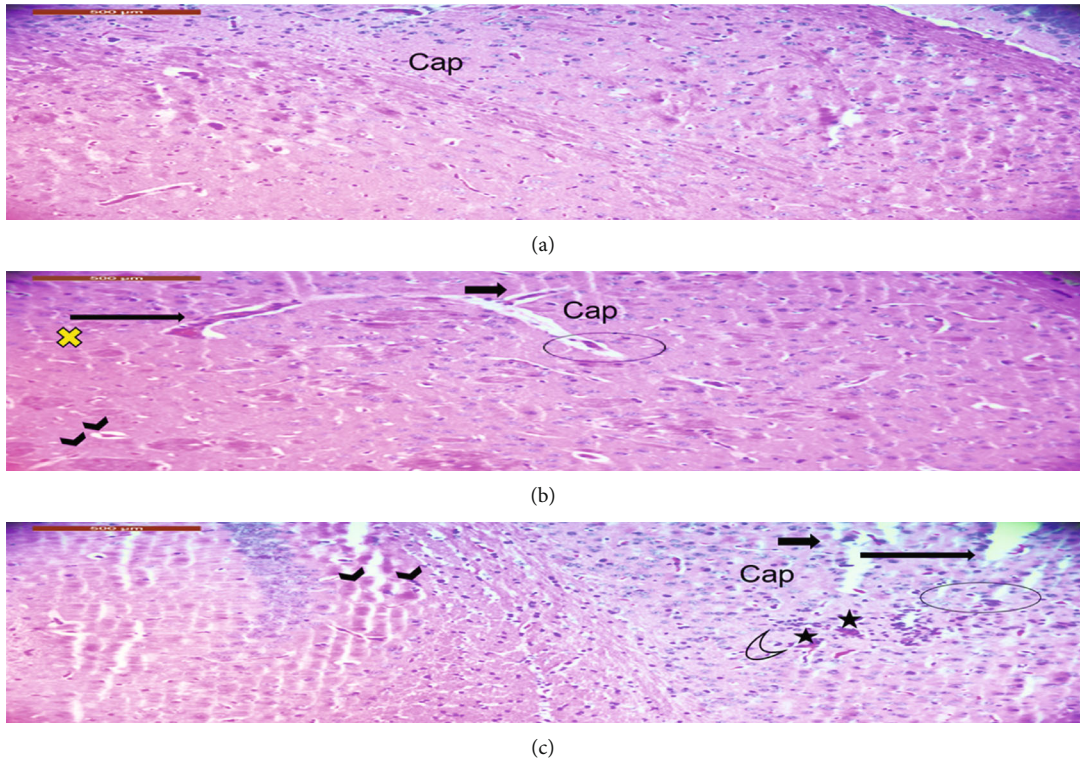

Figure 3: Histological findings of brain tissues stained with hematoxylin-eosin (HE) in rats using light microscopy. (a) The normal (control group) rat brain showed a uniform and normal arrangement and structure of cerebral capillaries (capillary structure, Cap) and blood vessels with normal configuration. (b) The L group (low13-RA dose) showed an increase in glycolipids (yellow x sign), congestion of cerebral blood vessels (short wide small arrow), and focal hemorrhage (long arrow). The hippocampal neurons were reduced to ghost cells, with no nuclear staining and a barely visible cell outline plus softening and hemorrhage (chevron arrows). (c) The H group (high dose) showed necrosis of neurons (small stars), neuronophagia (small circles), and neuronal edema (small crescent shape). Subarachnoid hemorrhage was also seen.

have a role in depression in a number of studies [54–56]. Besides, this agrees with many studies that reported prominent histopathological changes in the brain following 13-RA and in a dosed manner [57, 58]. The results insinuate that the mechanism behind 13-RA induced depression could be from the ability of the drug to inhibit neurogenesis. This study therefore agrees with several studies that showed histological changes of reductions in the density and size of neurons (neuronal atrophy) and dysfunctional neuronal circuits in the hippocampus and prefrontal cortex [59, 60] in major depression. Different alterations of the regional distribution of ^{99m}Tc-HMPAO retention have been reported in depressed patients [61]. Many clinical studies showed that 13-RA causes stress manifested by somatic intracranial hypertension, cerebral infarction, cerebral or thrombotic hemorrhage [62, 63], encephalopathy [64], brain blood vessel inflammation [65], and neurodegenerative disorders [66].

The correlation between brain perfusion and stress is also evident in the experimental results. The findings of this study show that 13-RA caused depression-like behavior in rats following the modified unpredictable mild stress model. This also agrees with many studies, which proved a strong relationship between 13-RA treatment and depression-like behavior [25]. In general, the relationship between stress and depression is well established [67, 68]. It was reported that the pathophysiology of the appearance of depressive symptoms after 13-RA administration in the rat mild stress model is linked to the dysfunctional GABAergic inhibitory system. This system is able to suppress the hippocampal cell division and hippocampal-dependent learning [61]. In addition, this was confirmed impairing the explicit memory and learning and at doses likely to produce serum levels within the range typically used to treat acne in humans [62] in some studies. These studies report that the retention in the brain is proportional to the CBF and is related to both the local hemodynamics status and the cellular content of a reduced glutathione, which reflects the amount of cellular injury or stress [68], the oxidative stress [69, 70], and the psychosocial stress. One study reported a strong association between psychological stress and CBF damage. Induced stress in mice produced cerebrovascular microbleeds in scattered locations, vascular pathology, and blood-brain barrier (BBB) breakdown. Similarly, some studies reported that 13-RA can pass the BBB and confirmed visualizing plasma immunoglobulins and erythrocytes within the parenchyma and perivascular spaces of mouse brains and high gene expression profiles during and after vascular disruptions due to stress [71].

Another major finding from our study is that the gradual increment vasodilation of blood flow to rat brain after 13-RA administration occurred in a dose-dependent manner. This was proved y analyzing stress. In physiology, stress causes the body to act in two directions: the first direction

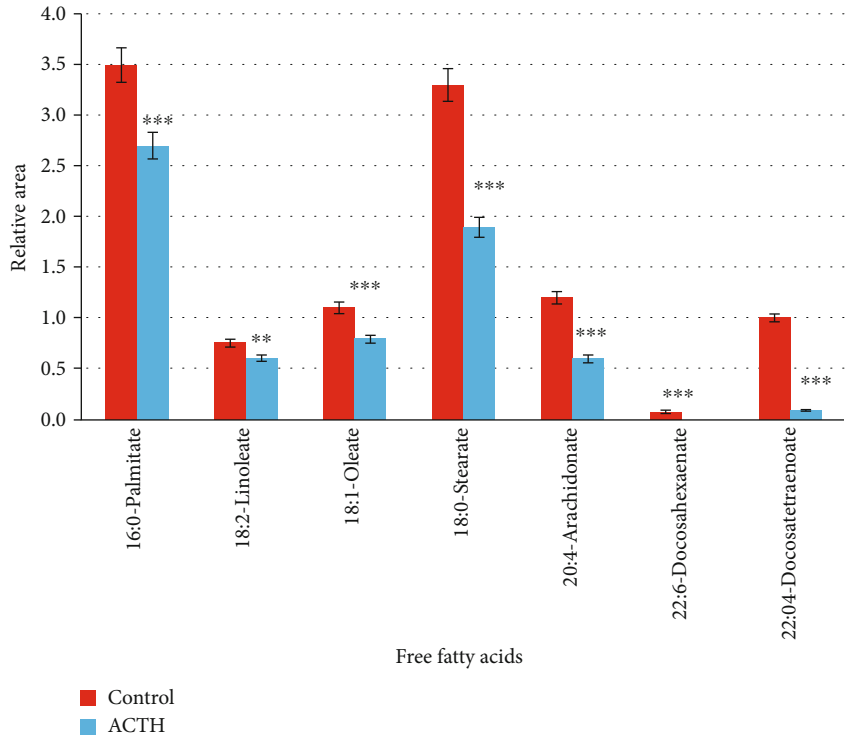

Figure 4: GC/MS results of free fatty acids extracted from the control and adrenocorticotropic hormone (ACTH) adrenals. Values are expressed as mean ± standard deviation. $^{***}p < .0001$ and $^{**}p < .001$ vs. control. $p < .05$ was considered statistically significant.

is the nervous system, such as the perception at the level of the brain, and the second direction is the endocrine system. One study presented a link between stress and neurovascular coupling, a physiological process that drives changes in blood flow to specific brain regions. The hemodynamic response function showed an increased signal in several brain regions, including in the temporal and prefrontal cortex, indicating changes in blood flow regulation in response to stress as well as the cortisol secretion and the adrenocorticotropic hormone (ACTH) response [72]. The ACTH is a hormone made by the pituitary gland, a small gland located at the bottom of the brain. ACTH controls the appearance of another hormone known as cortisol. Cortisol is formed by the adrenal glands, two small glands based above the kidneys. Cortisol provides an essential lead to respond to stress and regulate the use of food and energy or body metabolism.

In this study, we proved that ACTH prompts the adrenal cortex to release corticoids (glucocorticoids and mineralocorticoids) for energy by converting glycogen to glucose (glycogenolysis) and by breaking down fat into fatty acids and glycerol (lipolysis). Just like steroids, glucocorticoids and mineralocorticoids are the driving forces and the trigger for many neuropsychiatric symptoms, effects, and disorders, such as depression, quirk, mania, raving, hallucination, agitation, and even a sevenfold increased suicide or attempt average after the release of steroids [73, 74]. In our study, the mechanism of brain perfusion changes is due to the release of steroids. This is in agreement with one study associated between the presence of glucocorticoids and changes in brain volume and white matter microstructure [75]. Another study confirmed a strong association between the presence of glucocorticoids and the local vasodilation of spinal cord [76]. ACTH could also have caused the mobilization of free fatty acids and the vasodilation of the brain in our study.

Brain imaging results from this study also illustrate that 13-RA causes vasodilation. This phenomenon suggests a release of catecholamines for a few seconds to accelerate the vasodilatation of arteries throughout the working muscles and the brain. Catecholamines are also involved in stress responses. A unique observation from this study was the response of HPA axis stimulation to stress. The free fatty acids were consumed after 13-RA administration, and the free fatty acids were reduced significantly in the experimental groups in comparison with C. This agrees with the results of several studies that observed that ACTH and pituitary hormones stimulated the reduction of free fatty acid concentration in a dose-dependent manner and increased their consumption by the muscles during activity [58, 77]. The reduction in free fatty acid level was reported to cause a stimulatory effect on ACTH and the cortisol secretion [78, 79]. However, some studies reported that there was no effect of free fatty acids on ACTH and cortisol secretion in normal [80]. Since 13-RA causes mild suppression of pituitary hormone levels [77], the outcome of 13-RA treatment in humans might be directly related to altered steroid levels because of vasodilation in the blood circulation as explained above.

Moreover, this study points out the need to prevent the use of medications or drug mechanisms that may lead to

stress. Studies predispose subjects to an increased risk of suicide and depression after reduction in free fatty acids. 13-RA is strongly associated with stress. This agrees with our results. The highest ^{99m}Tc-HMPAO uptake counts were ordered from the highest to the lowest organ uptake and were in the brain, kidneys, heart, liver, gut, adrenals, lungs, testes, blood, and bones.

Many studies reported that 13-RA causes disruption in lipids such as dyslipidemia, hypertriglyceridemia [70], and imbalance in endocrine systems [81]. This study proves that free fatty acids are reduced due to depression and stress. Palmitate, a 16-carbon saturated fatty acid, is reduced in the brain after 13-RA administration due to stress formation and depression [82]. The linoleate, oleate, and stearate were reduced; some studies reported that this reduction is due to changes in the phospholipid formation [83]. Similarly, the arachidonate [84] and the docosahexaenoate were reduced and were reported due to depression [85]. The docosatetraenoate free fatty acids were reduced with unknown cause in comparison to the control group. The relationship of ACTH secretion and lipid levels is still unknown. Some studies reported that lipid levels have no effect on the ACTH secretion [86], while other studies reported that plasma lipid profile is affected by the ACTH [87, 88].

Therefore, our ^{99m}Tc-HMPAO imaging, behavioral, histological, and fatty acid experiments proved that the CBF is affected and increased by 13-RA. The study presented a rat model to detect the effect of 13-RA in causing stress such as depression using nuclear medicine imaging. Given that there has been an increasing incidence of depression and suicides in patients treated with 13-cis RA, the study has established how the drug affects neuronal signaling and the mechanism of action of neuroactive steroids and hormones to induce the disease. Results illustrate that the mechanism of action may affect and target the gamma-aminobutyric acid (GABA) receptors, which were reported to increase CBF and vasodilation in a dose-dependent manner. Findings that 13-cis RA increases brain perfusion to induce depression could help in the development of new antidepressants.

5. Conclusion

To our knowledge, this is the first study on the effects of 13-RA on rat brain using functional nuclear medicine imaging. Our findings suggest that 13-RA affects brain functioning by increasing blood flow to the brain and consuming free fatty acids, thus providing a possible biological mechanism by which 13-RA treatment could lead to depression and suicidal ideation in a minority of vulnerable acne patients. Studies using female rats and steroid levels to evaluate the effects of 13-RA on brain functioning are ongoing. Further investigation of the cerebral region that is most involved in the accumulation and uptake of ^{99m}Tc-HMPAO is needed, as well as which area in the brain is the most sensitive or is more specific for diagnosing the cerebral lobe pathology based on ^{99m}Tc-HMPAO. Besides, further analysis software coregistering ^{99m}Tc-HMPAO images to an MRI template will be under consideration.

Data Availability

The datasets generated in this study are available from the corresponding author upon reasonable request.

Conflicts of Interest

The authors have no conflict of interest.

Acknowledgments

We would like to acknowledge Kuwait University and King Faisal University for supporting this research using their facilities.

References

[1] Y.-H. Chen, W. M. Wang, C. H. Chung, C. H. Tsao, W. C. Chien, and C. T. Hung, "Risk of psychiatric disorders in patients taking isotretinoin: a nationwide, population-based, cohort study in Taiwan," *Journal of Affective Disorders*, vol. 296, pp. 277–282, 2022.

[2] C.-C. Draghici, R. G. Miulescu, R. C. Petca, A. Petca, M. Dumitrașcu, and F. Șandru, "Teratogenic effect of isotretinoin in both fertile females and males (Review)," *Experimental and Therapeutic Medicine*, vol. 21, no. 5, p. 534, 2021.

[3] W. Webster and H. Ritchie, "Teratogenic effects of alcohol and isotretinoin on craniofacial development: an analysis of animal models," *Journal of Craniofacial Genetics and Developmental Biology*, vol. 11, no. 4, pp. 296–302, 1991.

[4] O. Yilmaz Tasdelen, F. G. Yurdakul, S. Duran, and H. Bodur, "Isotretinoin-induced arthritis mimicking both rheumatoid arthritis and axial spondyloarthritis," *International Journal of Rheumatic Diseases*, vol. 18, no. 4, pp. 466–469, 2015.

[5] A. P. Rozin, O. Kagna, and Y. Shiller, "Sacroiliitis and severe disability due to isotretinoin therapy," *Rheumatology International*, vol. 30, no. 7, pp. 985-986, 2010.

[6] M. Daye, M. Belviranli, N. Okudan, I. Mevlitoglu, and M. Oz, "The effect of isotretinoin therapy on oxidative damage in rats," *Dermatologic Therapy*, vol. 33, no. 6, article e14111, 2020.

[7] J. Kaikati, S. Zoghaib, E. Kechichian et al., "The impact of acne treatment on quality of life and self-esteem: a prospective cohort study from Lebanon," *International Journal of Women's Dermatology*, vol. 7, no. 4, pp. 415–421, 2021.

[8] F. Kurhan and G. Z. Kamiş, "Isotretinoin induced psychotic mania: a case report," *Turk psikiyatri dergisi=Turkish journal of psychiatry*, vol. 32, no. 3, pp. 214–218, 2021.

[9] I. Ilić, N. Oršolić, E. Rođak et al., "The effect of high-fat diet and 13-cis retinoic acid application on lipid profile, glycemic response and oxidative stress in female Lewis rats," *PLoS One*, vol. 15, no. 9, article e0238600, 2020.

[10] H. U. Ozkol, H. Ozkol, A. S. Karadag, S. G. Bilgili, Y. Tuluce, and O. Calka, "Oral isotretinoin therapy of acne patients decreases serum paraoxonase-1 activity through increasing oxidative stress," *Drug and Chemical Toxicology*, vol. 38, no. 1, pp. 63–66, 2015.

[11] M.-L. Laroche, F. Macian-Montoro, L. Merle, and J. M. Vallat, "Cerebral ischemia probably related to isotretinoin," *Annals of Pharmacotherapy*, vol. 41, no. 6, pp. 1073–1076, 2007.

[12] S. A. Stuart, P. Butler, M. R. Munafò, D. J. Nutt, and E. S. J. Robinson, "A translational rodent assay of affective biases in depression and antidepressant therapy," *Neuropsychopharmacology*, vol. 38, no. 9, pp. 1625–1635, 2013.

[13] J. D. Bremner, K. D. Shearer, and P. J. McCaffery, "Retinoic acid and affective disorders: the evidence for an association," *The Journal of Clinical Psychiatry*, vol. 73, no. 1, pp. 37–50, 2012.

[14] O. Arican, S. Sasmaz, and O. Ozbulut, "Increased suicidal tendency in a case of psoriasis vulgaris under acitretin treatment," *Journal of the European Academy of Dermatology and Venereology*, vol. 20, no. 4, pp. 464-465, 2006.

[15] S. Trent, C. J. G. Drew, P. J. Mitchell, and S. J. Bailey, "Chronic treatment with 13-*cis*-retinoic acid changes aggressive behaviours in the resident-intruder paradigm in rats," *European Neuropsychopharmacology*, vol. 19, no. 12, pp. 876–886, 2009.

[16] K. R. Feingold, B. E. Brown, S. R. Lear, A. H. Moser, and P. M. Elias, "Localization of de novo sterologenesis in mammalian skin," *The Journal of Investigative Dermatology*, vol. 81, no. 4, pp. 365–369, 1983.

[17] E. García-Cruz and A. Alcaraz, "Testosterone deficiency syndrome: diagnosis and treatment," *Actas Urológicas Españolas*, vol. 44, no. 5, pp. 294–300, 2020.

[18] B. N. Zoob Carter, I. D. Boardley, and K. van de Ven, "The Impact of the COVID-19 pandemic on male strength athletes who use non-prescribed anabolic-androgenic steroids," *Frontiers in Psychiatry*, vol. 12, article 636706, 2021.

[19] M. V. Borgo, E. R. G. Claudio, F. B. Silva et al., "Hormonal therapy with estradiol and drospirenone improves endothelium-dependent vasodilation in the coronary bed of ovariectomized spontaneously hypertensive rats," *Brazilian Journal of Medical and Biological Research*, vol. 49, no. 1, article e4655, 2016.

[20] N. Z. Burger, O. Y. Kuzina, G. Osol, and N. I. Gokina, "Estrogen replacement enhances EDHF-mediated vasodilation of mesenteric and uterine resistance arteries: role of endothelial cell Ca^{2+}," *American Journal of Physiology. Endocrinology and Metabolism*, vol. 296, no. 3, pp. E503–E512, 2009.

[21] G. Pernod, G. Amalfitano, B. le Magueresse, F. Berger, B. Polack, and L. Kolodié, "Retinoids induced t-PA synthesis by C6 glioma cells–role in tumoral haemorrhagic necrosis," *Thrombosis and Haemostasis*, vol. 75, no. 2, pp. 332–338, 1996.

[22] I. Perić, V. Costina, P. Gass, P. Findeisen, and D. Filipović, "Hippocampal synaptoproteomic changes of susceptibility and resilience of male rats to chronic social isolation," *Brain Research Bulletin*, vol. 166, pp. 128–141, 2021.

[23] M. Tang, H. Huang, S. Li et al., "Hippocampal proteomic changes of susceptibility and resilience to depression or anxiety in a rat model of chronic mild stress," *Translational Psychiatry*, vol. 9, no. 1, p. 260, 2019.

[24] G. J. Quirk and J. S. Beer, "Prefrontal involvement in the regulation of emotion: convergence of rat and human studies," *Current Opinion in Neurobiology*, vol. 16, no. 6, pp. 723–727, 2006.

[25] A. Q. Song, B. Gao, J. J. Fan et al., "NLRP1 inflammasome contributes to chronic stress-induced depressive-like behaviors in mice," *Journal of Neuroinflammation*, vol. 17, no. 1, p. 178, 2020.

[26] L. Si, L. Xiao, Y. Xie et al., "Social isolation after chronic unpredictable mild stress perpetuates depressive-like behaviors, memory deficits and social withdrawal via inhibiting ERK/KEAP1/NRF2 signaling," *Journal of Affective Disorders*, vol. 324, pp. 576–588, 2023.

[27] C. Suzuki, S. Kimura, M. Kosugi, and Y. Magata, "Quantitation of rat cerebral blood flow using ^{99m}Tc- HMPAO," *Nuclear Medicine and Biology*, vol. 47, pp. 19–22, 2017.

[28] J. Mejia, A. C. C. Miranda, A. C. R. Durante et al., "Preclinical molecular imaging: development of instrumentation for translational research with small laboratory animals," *Einstein (São Paulo)*, vol. 14, no. 3, pp. 408–414, 2016.

[29] P. Bascuñana, B. J. Wolf, I. Jahreis et al., "(99m)Tc-HMPAO SPECT imaging reveals brain hypoperfusion during status epilepticus," *Metabolic Brain Disease*, vol. 36, no. 8, pp. 2597–2602, 2021.

[30] A. G. Ceulemans, S. Hernot, T. Zgavc et al., "Serial semiquantitative imaging of brain damage using micro-SPECT and micro-CT after endothelin-1-induced transient focal cerebral ischemia in rats," *Journal of Nuclear Medicine*, vol. 52, no. 12, pp. 1987–1992, 2011.

[31] E. M. Kim, H. J. Jeong, S. T. Lim, and M. H. Sohn, "Analysis of cell fraction of (99)mTc-HMPAO radiolabeled leukocytes," *Current Radiopharmaceuticals*, vol. 13, no. 2, pp. 142–148, 2020.

[32] S. Paakkinen, M. Vorne, T. Lantto, R. Mokka, and S. Sakki, "Detection of inflammation with 99mTC-HMPAO labelled leucocytes," *Annales Chirurgiae et Gynaecologiae*, vol. 76, no. 4, pp. 197–200, 1987.

[33] S. Zerarka, L. Pellerin, D. Slosman, and P. J. Magistretti, "Astrocytes as a predominant cellular site of (99m)Tc-HMPAO retention," *Journal of Cerebral Blood Flow and Metabolism*, vol. 21, no. 4, pp. 456–468, 2001.

[34] S. L. Hale, M. T. Vivaldi, and R. A. Kloner, "Fluorescent microspheres: a new tool for visualization of ischemic myocardium in rats," *The American Journal of Physiology*, vol. 251, 4, Part 2, pp. H863–H868, 1986.

[35] A. A. B. Eşrefoğlu, H. Elbe, E. Taşlidere, A. Cetin, and B. Ateş, "Melatonin is effective in reducing stress-induced organ damage in Wistar albino rats," *Turkish Journal of Biology*, vol. 38, pp. 493–501, 2014.

[36] X. J. Liu, Z. Y. Li, Z. F. Li et al., "Urinary metabonomic study using a CUMS rat model of depression," *Magnetic Resonance in Chemistry*, vol. 50, no. 3, pp. 187–192, 2012.

[37] H. Dong, Z. Gao, H. Rong, M. Jin, and X. Zhang, "β-asarone reverses chronic unpredictable mild stress-induced depression-like behavior and promotes hippocampal neurogenesis in rats," *Molecules*, vol. 19, no. 5, pp. 5634–5649, 2014.

[38] L. Duan, R. Fan, T. Li et al., "Metabolomics analysis of the prefrontal cortex in a rat chronic unpredictable mild stress model of depression," *Frontiers in Psychiatry*, vol. 13, article 815211, 2022.

[39] P. Willner, A. Towell, D. Sampson, S. Sophokleous, and R. Muscat, "Reduction of sucrose preference by chronic unpredictable mild stress, and its restoration by a tricyclic antidepressant," *Psychopharmacology*, vol. 93, no. 3, pp. 358–364, 1987.

[40] J. Xia, H. Wang, C. Zhang et al., "The comparison of sex differences in depression-like behaviors and neuroinflammatory changes in a rat model of depression induced by chronic stress," *Frontiers in Behavioral Neuroscience*, vol. 16, article 1059594, 2022.

[41] S. T. Ingalls, M. S. Kriaris, Y. Xu, D. W. DeWulf, K. Y. Tserng, and C. L. Hoppel, "Method for isolation of non-esterified fatty

acids and several other classes of plasma lipids by column chromatography on silica gel," *Journal of Chromatography*, vol. 619, no. 1, pp. 9–19, 1993.

[42] S. Meier, S. A. Mjøs, H. Joensen, and O. Grahl-Nielsen, "Validation of a one-step extraction/methylation method for determination of fatty acids and cholesterol in marine tissues," *Journal of Chromatography A*, vol. 1104, no. 1-2, pp. 291–298, 2006.

[43] I. W. Duncan, P. H. Culbreth, and C. A. Burtis, "Determination of free, total, and esterified cholesterol by high-performance liquid chromatography," *Journal of Chromatography*, vol. 162, no. 3, pp. 281–292, 1979.

[44] M. Hennebelle, R. K. Morgan, S. Sethi et al., "Linoleic acid-derived metabolites constitute the majority of oxylipins in the rat pup brain and stimulate axonal growth in primary rat cortical neuron-glia co-cultures in a sex-dependent manner," *Journal of Neurochemistry*, vol. 152, no. 2, pp. 195–207, 2020.

[45] Y. Wakabayashi, M. Uchiyama, H. Daisaki, M. Matsumoto, M. Sakamoto, and K. Kashikura, "Investigation of the new non-invasive semi-quantitative method of 123I-IMP pediatric cerebral perfusion SPECT," *PLoS One*, vol. 15, no. 11, article e0241987, 2020.

[46] Y. Y. Shih, B. H. de la Garza, S. Huang, G. Li, L. Wang, and T. Q. Duong, "Comparison of retinal and cerebral blood flow between continuous arterial spin labeling MRI and fluorescent microsphere techniques," *Journal of Magnetic Resonance Imaging*, vol. 40, no. 3, pp. 609–615, 2014.

[47] P. Abbona, Y. Zhao, L. Hubbard, S. Malkasian, B. Flynn, and S. Molloi, "Absolute cerebral blood flow: assessment with a novel low-radiation-dose dynamic CT perfusion technique in a swine model," *Journal of Neuroradiology*, vol. 49, no. 2, pp. 173–179, 2022.

[48] T. Başoglu, T. Ozbenli, I. Bernay et al., "Demonstration of frontal hypoperfusion in benign exertional headache by technetium-99m-HMPAO SPECT," *Journal of Nuclear Medicine*, vol. 37, no. 7, pp. 1172–1174, 1996.

[49] V. Di Piero, F. Fiacco, D. Tombari, and P. Pantano, "Tonic pain: a SPET study in normal subjects and cluster headache patients," *Pain*, vol. 70, no. 2, pp. 185–191, 1997.

[50] J. Olesen, L. Friberg, T. S. Olsen et al., "Timing and topography of cerebral blood flow, aura, and headache during migraine attacks," *Annals of Neurology*, vol. 28, no. 6, pp. 791–798, 1990.

[51] F. Hugo, B. van Heerden, N. Zungu-Dirwayi, and D. J. Stein, "Functional brain imaging in obsessive-compulsive disorder secondary to neurological lesions," *Depression and Anxiety*, vol. 10, no. 3, pp. 129–136, 1999.

[52] A. B. Newberg, M. Serruya, A. Gepty et al., "Clinical comparison of 99mTc exametazime and 123I Ioflupane SPECT in patients with chronic mild traumatic brain injury," *PLoS One*, vol. 9, no. 1, article e87009, 2014.

[53] E. Vanninen, J. T. Kuikka, M. Äikiä, M. Könönen, and R. Vanninen, "Heterogeneity of cerebral blood flow in symptomatic patients undergoing carotid endarterectomy," *Nuclear Medicine Communications*, vol. 24, no. 8, pp. 893–900, 2003.

[54] O. Ates, S. Cayli, E. Altinoz et al., "Neuroprotection by resveratrol against traumatic brain injury in rats," *Molecular and Cellular Biochemistry*, vol. 294, no. 1-2, pp. 137–144, 2007.

[55] R. S. Duman, G. R. Heninger, and E. J. Nestler, "A molecular and cellular theory of depression," *Archives of General Psychiatry*, vol. 54, no. 7, pp. 597–606, 1997.

[56] J. D. Bremner, M. Narayan, E. R. Anderson, L. H. Staib, H. L. Miller, and D. S. Charney, "Hippocampal volume reduction in major depression," *The American Journal of Psychiatry*, vol. 157, no. 1, pp. 115–118, 2000.

[57] A. B. Goodman, "Chromosomal locations and modes of action of genes of the retinoid (vitamin a) system support their involvement in the etiology of schizophrenia," *American Journal of Medical Genetics*, vol. 60, no. 4, pp. 335–348, 1995.

[58] V. Korkach and A. Iurchenko, "Concentration of free fatty acids in muscle following administration of corticotropin and hydrocortisone," *Biulleten'Eksperimental'noi Biologii i Meditsiny*, vol. 85, no. 2, pp. 161–164, 1978.

[59] G. Rajkowska, J. J. Miguel-Hidalgo, J. Wei et al., "Morphometric evidence for neuronal and glial prefrontal cell pathology in major depression," *Biological Psychiatry*, vol. 45, no. 9, pp. 1085–1098, 1999.

[60] R. M. Sapolsky, "The possibility of neurotoxicity in the hippocampus in major depression: a primer on neuron death," *Biological Psychiatry*, vol. 48, no. 8, pp. 755–765, 2000.

[61] A. Gardner, D. Salmaso, D. Nardo et al., "Mitochondrial function is related to alterations at brain SPECT in depressed patients," *CNS Spectrums*, vol. 13, no. 9, pp. 805–814, 2008.

[62] J. Crandall, Y. Sakai, J. Zhang et al., "13-cis-retinoic acid suppresses hippocampal cell division and hippocampal-dependent learning in mice," *Proceedings of the National Academy of Sciences of the United States of America*, vol. 101, no. 14, pp. 5111–5116, 2004.

[63] A. O. Varoglu and A. Aksoy, "Herpes simplex encephalitis and pseudotumour cerebri due to ısotretinoin," *The Journal of the Pakistan Medical Association*, vol. 68, no. 12, pp. 1833–11835, 2018.

[64] M. M. Dopheide and R. E. Morgan, "Isotretinoin (13-*cis*-retinoic acid) alters learning and memory, but not anxiety-like behavior, in the adult rat," *Pharmacology Biochemistry and Behavior*, vol. 91, no. 2, pp. 243–251, 2008.

[65] Y. D. Fragoso, N. S. Campos, B. F. Tenrreiro, and F. J. Guillen, "Systematic review of the literature on vitamin a and memory," *Dementia & Neuropsychologia*, vol. 6, no. 4, pp. 219–222, 2012.

[66] M. Maes, P. Galecki, Y. S. Chang, and M. Berk, "A review on the oxidative and nitrosative stress (O&NS) pathways in major depression and their possible contribution to the (neuro)degenerative processes in that illness," *Progress in Neuro-Psychopharmacology & Biological Psychiatry*, vol. 35, no. 3, pp. 676–692, 2011.

[67] T. A. Kimbrell, T. A. Ketter, M. S. George et al., "Regional cerebral glucose utilization in patients with a range of severities of unipolar depression," *Biological Psychiatry*, vol. 51, no. 3, pp. 237–252, 2002.

[68] S. H. Audi, E. R. Jacobs, P. Taheri, S. Ganesh, and A. V. Clough, "Assessment of protection offered by the NRF2 pathway against Hyperoxia-induced acute lung injury in NRF2 knockout rats," *Shock*, vol. 57, no. 2, pp. 274–280, 2022.

[69] C. Chen, S. Nakagawa, Y. An, K. Ito, Y. Kitaichi, and I. Kusumi, "The exercise-glucocorticoid paradox: how exercise is beneficial to cognition, mood, and the brain while increasing glucocorticoid levels," *Frontiers in Neuroendocrinology*, vol. 44, pp. 83–102, 2017.

[70] S. Gustafson, C. Vahlquist, L. Sjöblom, A. Eklund, and A. Vahlquist, "Metabolism of very low density lipoproteins in rats with isotretinoin (13-cis retinoic acid)-induced

hyperlipidemia," *Journal of Lipid Research*, vol. 31, no. 2, pp. 183–190, 1990.

[71] M. L. Lehmann, C. N. Poffenberger, A. G. Elkahloun, and M. Herkenham, "Analysis of cerebrovascular dysfunction caused by chronic social defeat in mice," *Brain, Behavior, and Immunity*, vol. 88, pp. 735–747, 2020.

[72] I. G. Elbau, B. Brücklmeier, M. Uhr et al., "The brain's hemodynamic response function rapidly changes under acute psychosocial stress in association with genetic and endocrine stress response markers," *Proceedings of the National Academy of Sciences of the United States of America*, vol. 115, no. 43, pp. E10206–e10215, 2018.

[73] L. Fardet, I. Petersen, and I. Nazareth, "Suicidal behavior and severe neuropsychiatric disorders following glucocorticoid therapy in primary care," *The American Journal of Psychiatry*, vol. 169, no. 5, pp. 491–497, 2012.

[74] L. L. Judd, P. J. Schettler, E. S. Brown et al., "Adverse consequences of glucocorticoid medication: psychological, cognitive, and behavioral effects," *The American Journal of Psychiatry*, vol. 171, no. 10, pp. 1045–1051, 2014.

[75] M. van der Meulen, J. M. Amaya, O. M. Dekkers, and O. C. Meijer, "Association between use of systemic and inhaled glucocorticoids and changes in brain volume and white matter microstructure: a cross-sectional study using data from the UK biobank," *BMJ Open*, vol. 12, no. 8, article e062446, 2022.

[76] W. Young and E. S. Flamm, "Effect of high-dose corticosteroid therapy on blood flow, evoked potentials, and extracellular calcium in experimental spinal injury," *Journal of Neurosurgery*, vol. 57, no. 5, pp. 667–673, 1982.

[77] A. S. Karadag, Z. Takci, D. T. Ertugrul, S. G. Bilgili, R. Balahoroglu, and M. Takir, "The effect of different doses of isotretinoin on pituitary hormones," *Dermatology*, vol. 230, no. 4, pp. 354–359, 2015.

[78] F. Lanfranco, R. Giordano, M. Pellegrino et al., "Free fatty acids exert an inhibitory effect on adrenocorticotropin and cortisol secretion in humans," *The Journal of Clinical Endocrinology and Metabolism*, vol. 89, no. 3, pp. 1385–1390, 2004.

[79] I. Sarel and E. P. Widmaier, "Stimulation of steroidogenesis in cultured rat adrenocortical cells by unsaturated fatty acids," *The American Journal of Physiology*, vol. 268, no. 6, Part 2, pp. R1484–R1490, 1995.

[80] K. Mai, T. Bobbert, V. Kullmann et al., "No effect of free fatty acids on adrenocorticotropin and cortisol secretion in healthy young men," *Metabolism*, vol. 55, no. 8, pp. 1022–1028, 2006.

[81] A. Abdelhamed, R. Ezz el-Dawla, A. S. Karadag, N. F. Agamia, and B. C. Melnik, "The impact of isotretinoin on the pituitary-ovarian axis: an interpretative review of the literature," *Reproductive Toxicology*, vol. 104, pp. 85–95, 2021.

[82] H. Liu, J. Pu, Q. Zhou, L. Yang, and D. Bai, "Peripheral blood and urine metabolites and biological functions in post-stroke depression," *Metabolic Brain Disease*, vol. 37, no. 5, pp. 1557–1568, 2022.

[83] R. S. Chapkin, B. Haberstroh, T. Liu, and B. J. Holub, "Characterization of the individual phospholipids and their fatty acids in serum and high-density lipoprotein of the renal patient on long-term maintenance hemodialysis," *The Journal of Laboratory and Clinical Medicine*, vol. 101, no. 5, pp. 726–735, 1983.

[84] Y. Nagayasu, D. Fujita, A. Daimon et al., "Possible prevention of post-partum depression by intake of omega-3 polyunsaturated fatty acids and its relationship with interleukin 6," *The Journal of Obstetrics and Gynaecology Research*, vol. 47, no. 4, pp. 1371–1379, 2021.

[85] T. Larrieu and S. Layé, "Food for mood: relevance of nutritional Omega-3 fatty acids for depression and anxiety," *Frontiers in Physiology*, vol. 9, p. 1047, 2018.

[86] M. Skoog, M. Berggren-Söderlund, P. Nilsson-Ehle, and N. Xu, "Lipid synthesis and secretion in HepG2 cells is not affected by ACTH," *Lipids in Health and Disease*, vol. 9, no. 1, p. 48, 2010.

[87] X. He, P. Xue, X. Xu et al., "Short-term administration of ACTH improves plasma lipid profile and renal function in kidney transplant patients," *Transplantation Proceedings*, vol. 38, no. 5, pp. 1371–1374, 2006.

[88] U. E. Lang and S. Borgwardt, "Molecular mechanisms of depression: perspectives on new treatment strategies," *Cellular Physiology and Biochemistry*, vol. 31, no. 6, pp. 761–777, 2013.